Long Waves at Norfolk Island

By R. A. de Szoeke

Division of Fisheries and Oceanography
Technical Paper No. 31

Commonwealth Scientific and Industrial
Research Organization, Australia
1972

ISBN 0 643 00000 3

Printed by CSIRO, Melbourne

71.502-1150

LONG WAVES AT NORFOLK ISLAND*

By R. A. DE SZOEKE†

Abstract

The spectra of long-wave records taken at Norfolk I. (29°02′S., 167°56′E.) during the International Geophysical Year are presented. The spectra show no significant peaks in the frequency range studied (approximately 0.02–0.5 cycle/min). Changes in intensity were also studied, but were not obviously correlated with local tropical cyclone activity. A theoretical analysis, taking account of the topography, showed that the recorded long-wave activity at the island is not likely to be due to trapped sill waves. No definite conclusion could be reached on the origin of the long-wave activity.

I. INTRODUCTION

The term "long wave" is applied to waves whose lengths λ are at least an order of magnitude greater than the depth h of water over which they are propagating, i.e.

$$\lambda/h > 10\,. \tag{1}$$

At this extreme wavelength these waves have equal phase and group velocities given by

$$c = (gh)^{1/2}\,, \tag{2}$$

(g = acceleration due to gravity), which is independent of wavelength. Table 1 shows, for various depths of water, minimum wavelengths according to the long-wave criterion (1), as well as propagation velocities according to formula (2). From these are deduced the *minimum* periods of long waves in various depths. We shall be concerned with waves of periods 2–30 min. In this range, far below the period of rotation of the earth, Coriolis effects are negligible.

Now, propagation velocity is inversely proportional to refractive index in geometrical wave optics, so that, drawing the obvious analogy, long water waves can be refracted and totally internally reflected by depth variations in an exactly similar fashion to light waves in media of varying refractive indices. This has led to the investigation, both theoretical and practical, of the properties of long waves in the vicinity of large depth contrasts.

Snodgrass, Munk, and Miller (1962) and Buchwald (1968) have studied long waves on continental shelves and mid-oceanic ridges and postulated the existence of modes trapped by being totally internally reflected at the shelf boundary and reflected again at the shore (or at the other shelf boundary in case of an oceanic ridge). Munk, Snodgrass, and Gilbert (1964) demonstrated convincingly the existence of these trapped shelf waves by performing a spectral analysis of wave observations with respect to both

* Division of Fisheries and Oceanography, CSIRO, Reprint No. 703.

† Division of Fisheries and Oceanography, CSIRO, Cronulla, N.S.W.; present address: Oceanography Department, Nova University, College Avenue, Fort Lauderdale, Florida 33314, U.S.A.

time and space. This gave a spectral density field in the wavenumber–frequency plane which in the case of long waves on the Californian shelf agreed most strikingly with the dispersion relation predicted by theory.

Summerfield (1967) has reported some observations of long waves of about 6 min period with a 2 hr beat at Macquarie I. Prompted by this, Longuet-Higgins (1967) has studied theoretically the modes which can be trapped on a submerged circular sill in an infinite ocean.

During the International Geophysical Year a single wave recorder was installed at Norfolk I., primarily for the purpose of observing seismically generated wave disturbances (i.e. tsunamis). I have analysed parts of these records in an attempt to discover whether oscillations of the Longuet-Higgins type are present at the island.

TABLE 1

VELOCITY, MINIMUM WAVELENGTH, AND MINIMUM PERIOD FOR LONG WAVES

Depth (m)	Phase Velocity (m/sec)	Minimum Wavelength (m)	Minimum Period (sec)
10	9.9	100	10
50	22	500	23
100	31	1000	32
500	70	5000	71
1000	99	10000	101
5000	220	50000	230

Section II describes the wave data: the period of operation, type of instrument, location, the nature of the record, the digitization, the computation of spectra. Section III summarizes some of the features of the records and their spectra and suggests explanations of those features. Section IV examines the relevance to each other of the spectra obtained and the Longuet-Higgins theory of island-wave oscillations. The conclusions regarding this point were negative: nothing which could be unambiguously called a trapped island wave was observed; on the other hand, a theoretical argument is advanced to show that the effects of such island waves are expected to be very small at the island itself in the centre of its sill.

In Section V, the possibility of the impulsive generation by meteorologic disturbances of ridge-wave modes of the type postulated by Snodgrass, Munk, and Miller (1962) and Buchwald (1968) is examined. The theoretical form of the group of high activity associated with such an impulsive disturbance is discussed and compared with the groups observed in the records. The conclusion is negative: no wave groups with the properties which should be characteristic of ridge waves are evident.

Finally, because of the inconclusiveness of the present investigation, suggestions are made (Section VI) for observational programs to settle the main points of controversy raised here.

II. Data Analysis

Wave records were taken at Norfolk I. almost continuously during the period of the International Geophysical Year–International Geophysical Cooperation (August 1957 through December 1958) by the Geophysics Department of the Australian National

University (Jaeger 1960; Stacey 1961). The location of the recorder is shown in Figure 1; the bathymetry around Norfolk I. is shown in Figure 2. The instrument used was a Van Dorn portable tsunami recorder (Van Dorn 1956) which by a system of pneumatic filters reduced the large amplitudes of high frequency (wind-generated swell) and low frequency (tidal) components. The details of the relative amplitude

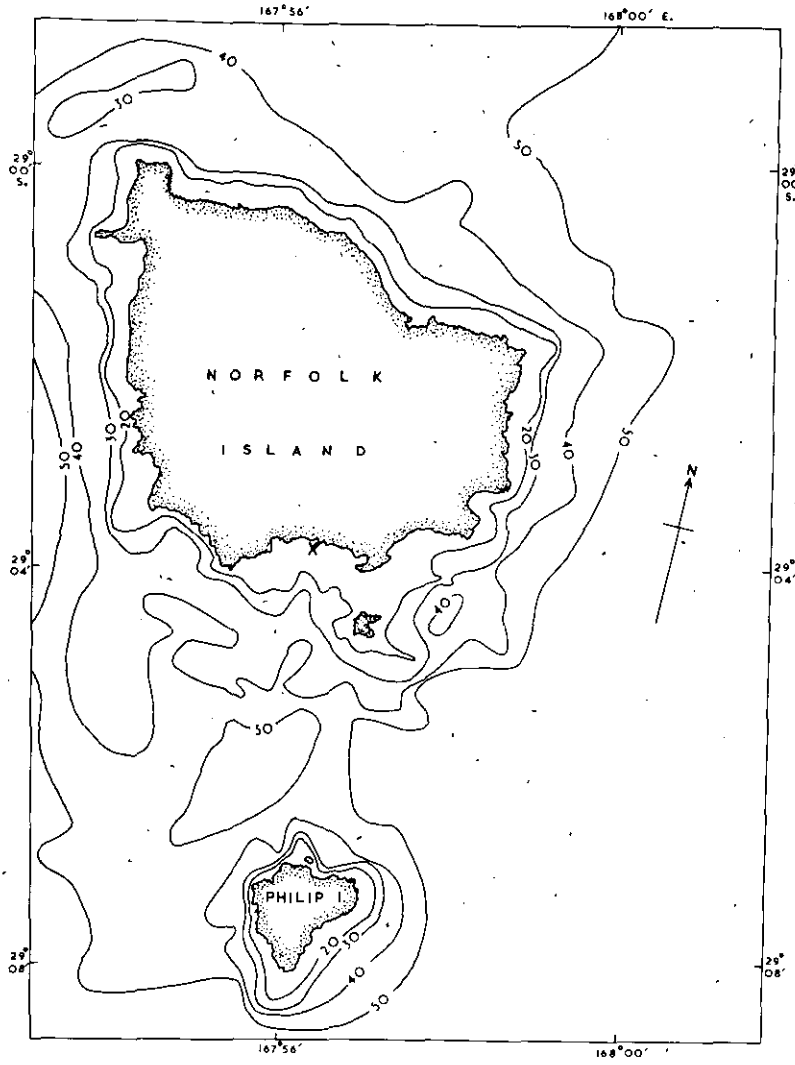

Fig. 1.—A map of Norfolk I. and surrounding waters with contoured depths in metres showing the location (X) of the wave-recorder.

response characteristics of this type of recorder are discussed more fully in Van Dorn's paper and by Munk, Iglesias, and Folsom (1948) but the effectiveness of the filtering is evident from a visual inspection of the records: the most prominent components are in the 4–20 min long-wave period band, while no activity at periods shorter than about 2 min is discernible; at the other end of the spectrum a slight 12-hourly drifting due to relics of the semidiurnal tide is apparent. The records have been traced on an Esterline Angus strip chart recorder at a chart speed of 6 in./hr. The height scale on the chart runs from 0 to 1 graduated in increments of 0.02, and, for lack of more satisfactory information on the calibration of the recorder it has been assumed that

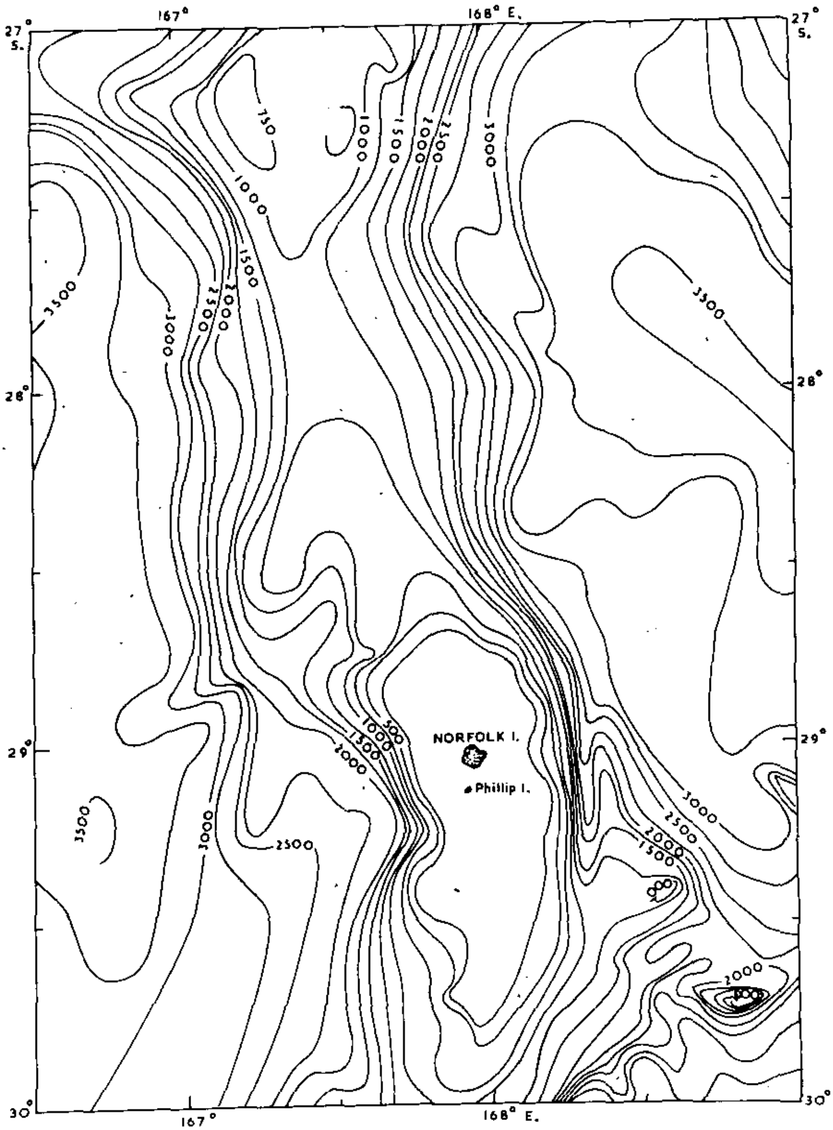

Fig. 2.–A larger scale map showing the bathymetry around Norfolk I. and its ridge.

one chart unit (c.u.) (i.e. the full chart displacement) represents about 10 cm of water height in the period range of maximum response (4–60 min). The possible inadequacy of this assumption, however, should be borne in mind.

Because of the apparent absence on visual inspection of components with periods less than 2 min, a sampling interval of 1 min was chosen for the digitization of the record. A Dobbie–MacInnes pencil-follower chart reader was used in the digitization. Because of the curved scale on the y-axis of the Esterline Angus chart and because the chart reader yields its output in Cartesian coordinates, transformation of coordinates and linear interpolation of the x-coordinate had to be performed to obtain the correct readings at equispaced time intervals. Points were read much more densely than the intended sampling interval with the pencil follower to minimize errors in this interpolation.

In all, about 20 days of record were read in this way; covering the periods 0931 hr February 12, 1958, to 2050 hr February 20, 1958, 1546 hr March 17, 1958, to 0230 hr March 23, 1958, 1016 hr August 11, 1958, to 1900 hr August 19, 1958 (with minor breaks) (Norfolk I. time). The first and third of these were chosen to represent summer and winter activity; the second segment was chosen because it coincided with a tropical cyclone (8C, Table 2) in the Fiji–New Caledonia area. The section of record 0001 hr August 17, 1958, to 1900 hr August 19, 1958, was analysed by Miss Elly Hoeve.

Because of availability of computer programs (Holsten and Groves 1966), the spectral analysis was carried out using the method of "faded overlapping segments" (FOS) with 50% overlap (see Groves and Hannan 1968 for a detailed discussion of this method, and Rosenblatt 1962 for a general exposition of the mathematical principles of time series analysis).

In this method, given a time series $x(n)$, $n = 1, 2, \ldots$, the overlapping segments mentioned are $\{x[m(j+1) + p], p = -m+1, \ldots m\}$, $j = 0, 1, 2, \ldots$, each of length $2m$. From each of these segments $m+1$ modulus-squared Fourier amplitudes are calculated by the formula

$$\xi_j(\alpha) = (1/4\pi m)\left|\sum_{p=-m+1}^{m} a(p)x(m(j+1)+p)e^{ip\alpha/m}\right|^2$$

for $\alpha = 0, 1, \ldots m$. The "fader" $a(p)$ is some normalized bell-shaped envelope or "window", such as the Lanczos-squared kernel.

$$\sqrt{3}\,\{\sin[\pi(2p-1)/(2m+1)]/[\pi(2p-1)/(2m+1)]\}^2\,,$$

or the cosine taper

$$\tfrac{1}{2}\{1+\cos[\pi(2p-1)/(2m+1)]\}\,,$$

which is applied to each segment. An estimate of the spectral density can be obtained by averaging for each frequency band, H of the squared amplitudes obtained above:

$$\hat{f}_H(\alpha) = (1/H)\sum_{j=0}^{H-1} \xi_j(\alpha)\,.$$

Assuming stationarity and a joint Gaussian distribution of the time series $x(n)$ the estimates $\hat{f}_H(\alpha)$ of the spectrum have a χ^2 distribution with $2H$ degrees of freedom, for the Lanczos-squared fader, and so confidence ranges can be assigned in the usual way. The crucial role of the fader windows is in minimizing the covariance between frequency bands of the spectral estimates. Roughly speaking, the smoother the fader, i.e. the more gently it attenuates the extremities of the segment, the less the correlation between neighbouring bands. Figure 3 is a plot of the normalized correlation between frequency bands α, α' as a (symmetric) function of $\alpha-\alpha'$ for the cosine taper contrasted with no fader at all ("Box-car" data window), i.e. $a(p) \equiv 1$. The efficacy of the fading is strikingly evident: for larger band separations than those shown the correlation falls off according to $\pi^{-2}(\alpha-\alpha')^{-6}$. The effect of the cosine taper has been shown in

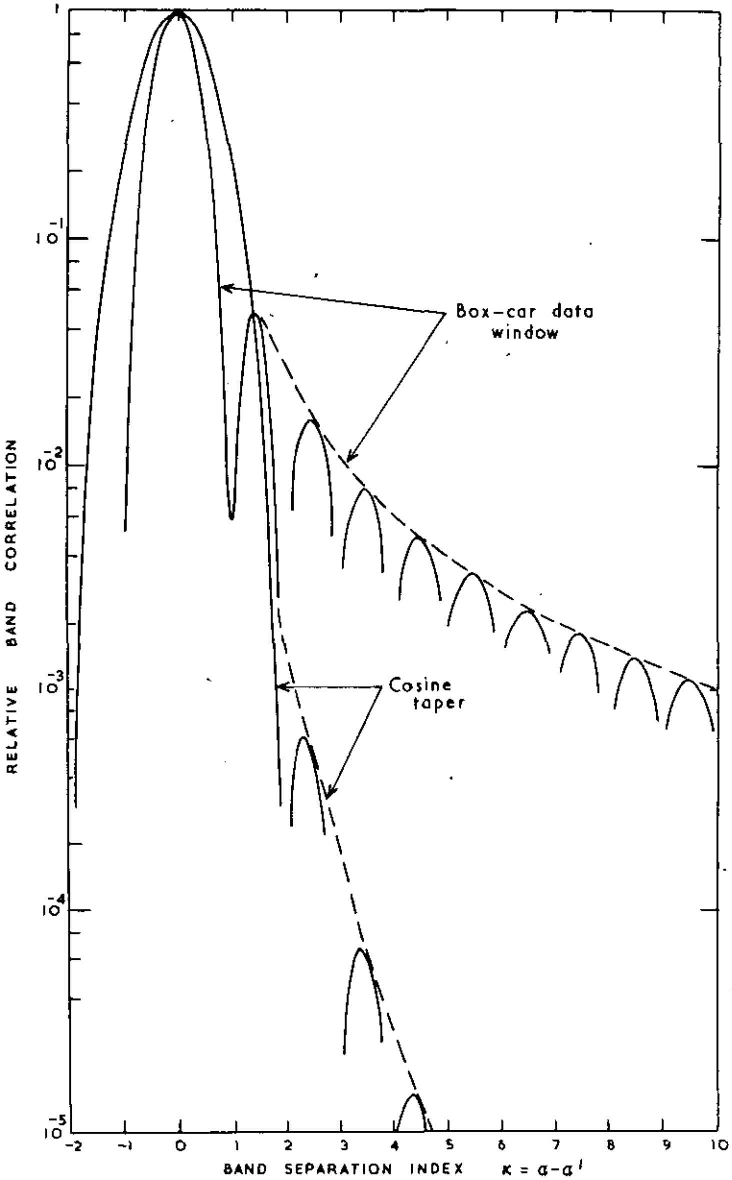

Fig. 3.–The spectral window of the cosine taper. The ordinate axis gives the normalized correlation between the frequency bands α and α' as a function of $\alpha-\alpha'$ on the abscissa.

Figure 3 because of the possibility of obtaining its frequency band correlation properties analytically. Unfortunately this is impossible with the Lanczos-squared fader which requires laborious numerical computation: nevertheless we expect its quantitative as well as qualitative properties to be similar or better (Groves and Hannan 1968).

This FOS method was used in the present situation with $m = 36$ so that, with a reading interval of 1 min [Nyquist frequency - 0.5 cycle/min (cpm)], spectral estimates were obtained for bands centred at $(0.5/36)\alpha = 0.014\alpha$ cpm, $\alpha = 0, 1, ..., 36$. The tidal residual mentioned earlier can be as high as 0.2–0.3 c.u. in crest-to-trough amplitude (representing an amplitude attenuation by the instrument of order 10^{-2}) compared with a range of 0.02–0.8 c.u. for the 4–20 min band. Clearly care is necessary to ensure that even this small tidal relic does not contaminate spectral estimates in neighbouring frequency bands.

Inspection of the analyses reveals spectral densities typically in the 10^{-2}–10^{-1} c.u.^{2}/cpm range for the 0th frequency band, caused by the tidal and other long-period residuals together with instrumental drift. If the cosine taper is used, Figure 3 then leads us to expect, in the second band, contamination of order 10^{-4}–10^{-3} c.u.^{2}/cpm, and in the fourth band, 10^{-6}–10^{-5} c.u.^{2}/cpm. In fact, typical spectral densities for these bands are, respectively, 10^{-3}–10^{-2} and 10^{-4}–10^{-3} c.u.^{2}/cpm. The former is somewhat dubious but the latter completely acceptable vis-à-vis the likely contamination. We conclude that frequency bands higher than the second are uncontaminated by low frequency noise spillover.

As the other end of the frequency range, near the Nyquist frequency, we face the problem of aliasing. We note, however, that all the spectra obtained show a decline in spectral density with increasing frequency: typically, the spectra range over five orders of magnitude from the 0th to the 36th band. From this we infer that aliasing is unlikely to affect any but the highest two or three bands.

The visual reading error of the analogue trace on the chart is about 0.01 c.u., or half the finest graduation on the chart. We assume (perhaps incorrectly) that the noise level of the recorder is within similar bounds. The random noise due to digitization of the records is negligible by comparison. The total variance due to a random error of 0.01 c.u. will be $(0.01)^2$ c.u.^{2} distributed over the bandwidth of the spectrum, 0–0.5 cpm. The threshold noise level, per frequency band, we therefore estimate to be $(0.01)^2/(0.5\times36) \cong 0.5\times10^{-5}$ c.u.^{2}/cpm, or, using the assumed equivalence, 1 c.u. $\equiv$ 10 cm, 0.5×10^{-3} cm^2/cpm. Inspection of the spectra obtained reveals that, at the high frequencies, the energy density reaches to about this level, but rarely below. We conclude that, except for the highest two or three frequency bands, unreliable anyway because of aliasing, the spectral densities are usually above the threshold noise level.

Visual inspection of the chart records shows that the level of long-wave activity can wax and wane appreciably over time intervals as short as 12 hr. The records form a time series which is palpably non-stationary. To render the records at least quasi-stationary the number H of overlapping segments was chosen to be 10. This procedure yields four spectra for each day of record. The number of degrees of freedom is then 20, and limits of statistical confidence can be assigned, with the use of χ^2 tables. Such confidence limits are indicated on the spectra. Spectra of longer time series whose lengths are multiples of 6 hr can be obtained by averaging several successive individual 6-hourly spectra in the obvious way. This would yield greater statistical confidence, although problems of non-stationarity may arise.

The spectra so obtained are too numerous to display here in their entirety. They are on file at the CSIRO Division of Fisheries and Oceanography, together with the digitized records. We do show, however, the envelopes of all the records obtained (Fig. 4). The individual records are distributed fairly evenly between the two extremes although a little more densely towards the lower extreme. The plot is of spectral density in units of (c.u.)^2/(0.5 cpm) (≡ 200 cm^2/cpm, on the arbitrary conversion assumed above) on a logarithmic scale against frequency (0–0.5 cpm) on a linear scale. The lowest curve gives the lower bound of a group of 6-hourly spectra covering the

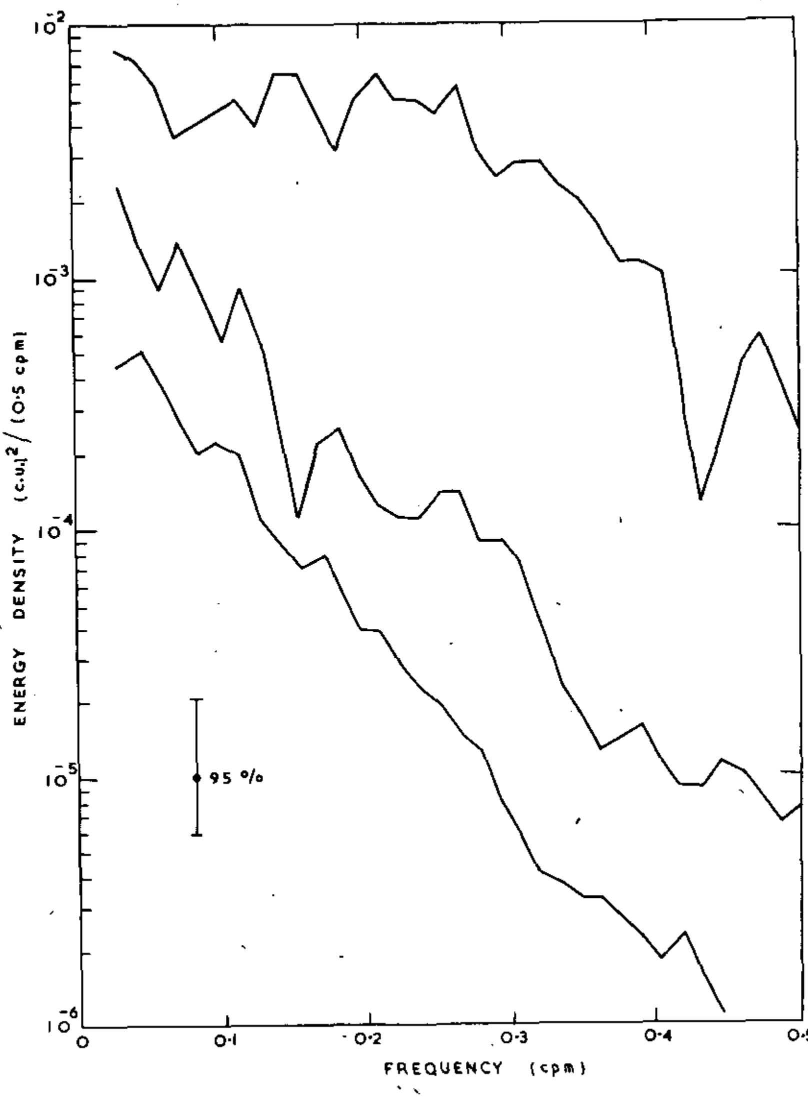

Fig. 4.–Typical 6-hourly spectra for the period 1201 hr February 12, 1958, to 2400 hr February 15, 1958. The lower spectrum is the lower bound of all the spectra during this period. The upper spectrum is the upper bound and also an example of a high-activity spectrum. The middle spectrum shows typical background activity. The 95% confidence limits are also shown.

period 1201 hr February 12, 1958, to 2400 hr February 15, 1958. The upper curve is a spectrum made during a burst of high wave activity on February 15, 1958; it also forms the upper bound of all the spectra. The middle curve is a typical example of a spectrum of the more usual background activity.

For reasons which are expounded in Section IV, spectral analysis was also carried out on much longer pieces of record at much higher frequency resolutions than used in the 6-hourly spectra. These high-resolution spectra are shown in Figures 9–14.

III. Discussion of Spectra

(a) General Features

The general features discernible in these 6-hourly spectra are:

(1) A decline in spectral density from low to high frequencies, typically covering two to three orders of magnitude.

(2) Bursts of quite intense wave activity lasting 1–2 days (2 cm visually estimated mean amplitude) intersperse the more usual and quieter activity (0.5–1.0 cm mean).

(3) At occasions of intense wave activity the spectral level rises over the entire frequency range but more markedly at higher frequencies (>0.2 cpm). The most remarkable such spectrum declines only about 1 order of magnitude in contrast with what is noted in item 1 above (see Fig. 4).

(4) No fine structure is evident in these records. Most fine-scale variations (i.e. structure extending over three to four adjacent spectral estimates from the 36 obtained in the frequency domain) are within the range of the 95% confidence limits, and those that are not do not reappear in spectra obtained from adjacent pieces of record. A similar remark can be made when higher frequency resolutions are used (Figs. 9–14).

(b) Activity Index

To investigate items (2) and (3) more thoroughly, an attempt was made to define an "index" of wave activity and to graph this index over several months. Two methods were used to avoid the labour of digitizing the records every minute. First, I attempted to scan the records noting every *third* crest-to-trough amplitude and performing a mean every 6 hr. When even this proved too laborious, a more mechanical method was devised using the pencil-follower whereby all discernible maxima and minima were read and differences between adjacent ones averaged over 6 hr. The combined results are shown in Figure 5 covering the period from June 17 to September 5, 1958, with breaks where the mean amplitudes (activity index) are plotted against time. Wind speeds at the island, estimates of which were available at 2300 hr of each day (Norfolk I. local time) are also plotted in Figure 5. No obvious relationship is apparent. Intense wave activity occurred on July 8–9, August 3–4, September 2–3. The activity for most of the second half of June maintained a relatively high level.

(c) *Relationship to Weather*

Tracks of tropical cyclones in the area during the 1957–58 season were perused (Newman and Bath 1959) and compared with the wave records. Table 2 lists the dates and areas of occurrence of type C tropical cyclones, the most intense variety according to a scale devised by the Meteorological Bureau, together with an indication of the level of long-wave activity according to visual estimation. Again, no clear connection is apparent. Cyclone 16C whose centre passed within 20 miles (32 km) of Norfolk I. coincided with moderate long-wave activity, but so did cyclone 8C far away in the Fiji–New Caledonia region. On the other hand, bursts of intense wave activity occurred at times when no obvious atmospheric cause is apparent.

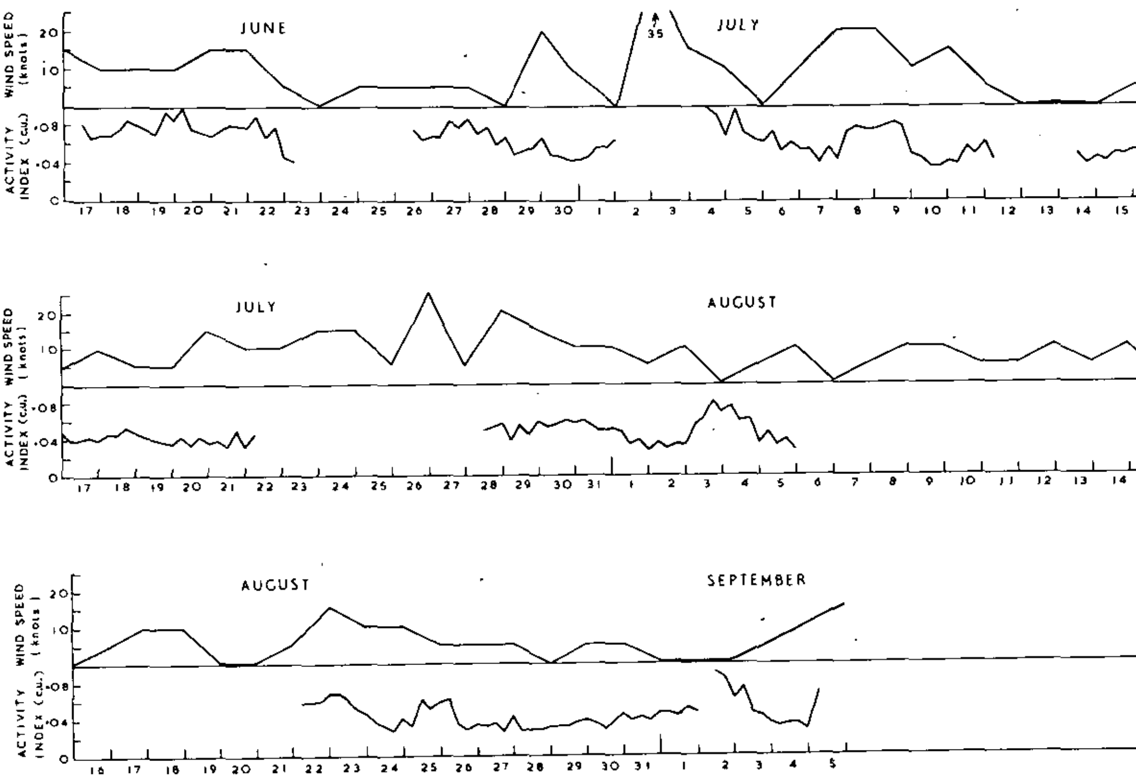

Fig. 5.—Activity index against daily wind speed for the period June 17–September 5, 1958.

(d) *Surf Beats*

A third explanation is that the bursts of intense activity are due to the phenomenon of surf beats (Munk 1949; Tucker 1950, Longuet-Higgins and Stewart 1962, 1964) which in effect are the amplitude envelope of the swell waves reflected from the beach at Norfolk I. at times of intense swell impinging on the island. This hypothesis is attractive because of the feature noted in item (3), that the high frequency end of the spectrum (periods less than 5 min) rises more in comparison with the low frequency end: this is in the period range of surf beating 1–10 min, as noted by the authors cited. However, owing to the absence of swell records of any kind, no check of this hypothesis is possible.

TABLE 2

DATES AND POSITIONS OF TROPICAL CYCLONES, 1957–1958 (AFTER NEWMAN AND BATH 1959)

+ indicates activity above 2 cm mean, – activity below 1 cm mean, *visually estimated*

Identification Number	Dates	Area	Wave Activity
3C	January 5–7, 1958	Ellis–Fiji–Kermadec	–
8C	March 11–17, 1958	Fiji to New Caledonia	+
12C	April 2–11, 1958	Solomons, New Hebrides, Fiji	–
14C	April 17–23, 1958	Solomons–central and south-eastern Coral Sea	–
15C	June 4–15, 1958	Solomons–central Coral Sea to east New Zealand	–
16C	June 19–22, 1958	South coast of Queensland–North Tasman Sea (passed within 20 miles of Norfolk I.)	+

(*e*) *Dispersion*

The hypothesis that the bursts of high activity may be caused by impulsive generation by moderate submarine seisms was examined (i.e. the long waves may be "small" tsunamis). Norfolk I. is only 1500–2000 km from the Tonga–Kermadec Trenches, regions of very high seismic activity.

Munk *et al.* (1963) have reported marked success in tracing the origins of well-developed swell by discerning the dispersion characteristics from the development of the spectra in time. Long waves are dispersive only at the second order so that this technique will not work as well. For the group velocity of a long wave of frequency f cpm is, up to the second order,

$$V(f) = (gh)^{1/2}[1 - (h/2g)(2\pi f)^2] .$$

The difference in arrival time between two frequencies f_1, $f_2 = f_1 + \Delta f$ from a source at distance L is, assuming constant intervening depth,

$$\begin{aligned} \Delta T = T_2 - T_1 &= L[1/V(f_2) - 1/V(f_1)] \\ &\doteqdot (-L/V_1^2)(\mathrm{d}V_1/\mathrm{d}f_1)\Delta f \\ &= L(2\pi)^2(h/g^3)^{1/2} f_1 \, \Delta f . \end{aligned}$$

For $h = 4000$ m, we have

$$(2\pi)^2 \, (h/g^3)^{1/2} \doteqdot 0.4 \ \mathrm{min}^3/\mathrm{km} .$$

If $f_1 = 0.2$ cpm, $\Delta f = 0.1$ cpm, and $L = 5000$ km, say, then $\Delta T \doteqdot 40$ min. This reasoning rules out distant impulsive generation of moderate intensity because the principal effects will pass a fixed point within a few hours at most, and at least 6 hr of record are required for statistically reliable spectral estimates. The exceptions are unusually powerful generators such as the Chilean earthquake of May 22, 1960, (Miller, Munk, and Snodgrass 1962) or the Alaskan earthquake of March 28, 1964 (Van Dorn 1965) whose associated tsunamis were easily discernible on tide recorders around the Pacific Ocean.

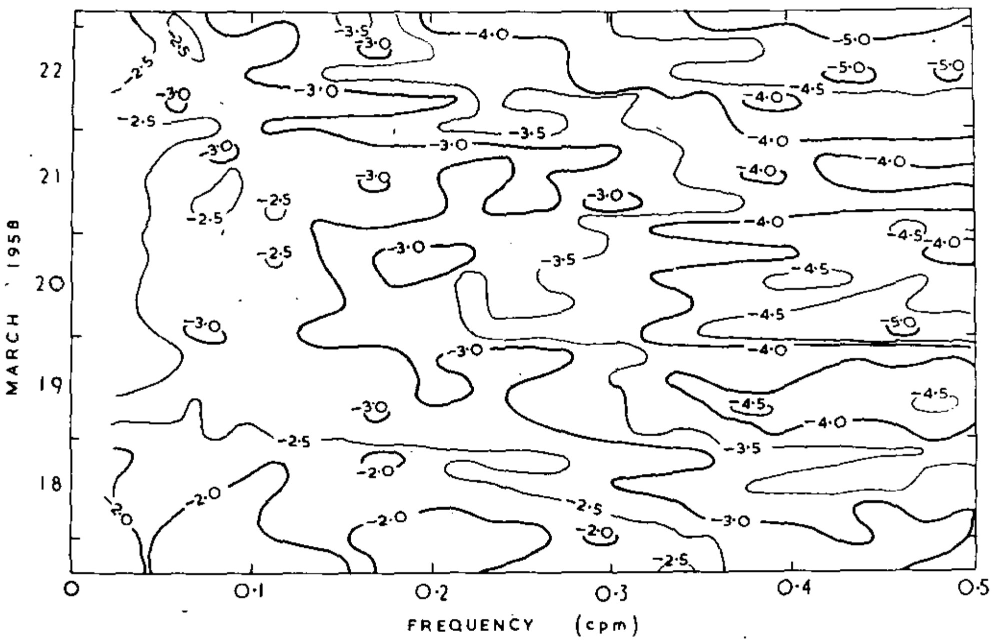

Fig. 6.—A contoured plot of the development of energy density in time for the period 1546 hr March 17, 1958, to 0230 hr March 23, 1958. The units on the contours are of $\log_{10}$ [energy density in $(\text{c.u.})^2/(0.5\ \text{cpm})$].

Nevertheless we have plotted the 6-hourly spectra discussed in Section II for the period 1546 hr March 17, 1958, to 0230 hr March 23, 1958, and contoured the quantity $\log_{10}$ [energy density in $(\text{c.u.})^2/(0.5\ \text{cpm})$] on the frequency–time plane in Figure 6. The only significant feature in this record is the declining trend with time of the spectral levels. The period up to about midnight, March 18, had been one of intense activity, possibly associated with cyclone 8C (Table 2), followed by the more usual quiescent activity. Figure 6 displays well the extremes encountered in all the spectra.

IV. Trapped Island-Sill Waves

Longuet-Higgins (1967) studied the problem of the oscillation of the water on a submerged circular sill. He discovered that no steady modes could exist, even in the inviscid case, because the system always radiated energy to infinity. However, for some modes the rate of this energy loss is minimal and it is possible that upon excitation these modes may persist long enough to be discernible in a long-wave record.

Let Figure 7 represent an instantaneous cross-section of the sill, radius a, through its centre. The free-surface elevation declines exponentially going outwards from the sill edge – similar to the exponential fringe accompanying trapped waves on straight ledges – until an outer critical radius r_2 is crossed beyond which it becomes oscillatory. This oscillatory region is the cause of the energy radiation to infinity, the rate of which is proportional to the square of the amplitude of oscillation at r_2: Clearly, the further r_2 is from a, the larger the intervening amplitude attenuation, and the less the rate of energy loss. Coming inwards from a, the surface elevation is oscillatory until an inner critical radius r_1 is reached where the solution again declines quasi-exponentially, becoming zero at the centre.

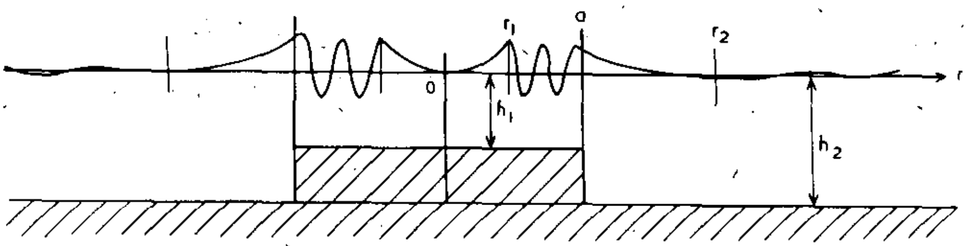

Fig. 7.–A cross-section through a diameter of the circular island used in Longuet–Higgins' model. A schematic plot of a possible trapped mode is given, showing its critical radii.

Table 3 is calculated from a similar table given by Longuet-Higgins (1967) and displays the natural frequencies ω and inverse damping factors (i.e. $1/e$ decay time due to energy radiation) for a sill of radius a = 40 km and depth h_1 = 200 m rising from an ocean of depth h_2 = 3200 m, so that h_1/h_2 = 1/16, which are taken to represent the Norfolk I. sill (Fig. 2). n is the polar wave number, being the number of wavelengths around the circumference of the sill. The critical radii are given by

$$r_i = n(gh_i)^{1/2}/\omega\,, \quad i = 1, 2 \tag{3}$$

for each mode. These also are given in Table 3 as a proportion of a. For comparison, the radius of Norfolk I. is about 1/10 of a.

Summerfield (1967) has studied the effect of a protuberant island, radius b, at the centre of the sill. If, for a given mode, as calculated above, $b < r_1$, that is, the island is within the region of low energy density due to the exponential amplitude decline, then the frequency and damping factor of that mode are not much affected by the presence of the island nor would a wave recorder at the island record much wave activity due to this mode. But if $b > r_1$, then the frequency and damping factor are increased and, more importantly, the wave activity due to the mode is more apparent at the island. This effect is achieved for small n; or large ω, which reduce r_1 (equation 3). But these same conditions reduce r_2 with a consequent increase in damping factor (cf. Table 1). One concludes that if the waters round the island are disturbed by the passage of a pulse, after which the modes are left to decay naturally, those modes most easily discernible at the island will decay in a short time of order roughly 1-2 hr. Since a minimum record length for the necessary frequency resolution combined with statistical reliability in a spectral analysis is about 6 hr, it is unlikely that the passage of any but an extremely powerful pulse will be felt in the wave records at Norfolk I.

TABLE 3

NATURAL FREQUENCIES, DECAY TIMES, AND CRITICAL RADII FOR OSCILLATIONS ON A SUBMERGED SILL

Polar Wave Number n	Frequency (cpm)	Decay Time (min)	Critical Radii	
			r_1	r_2
1	0.039	85	0.27	1.09
2	0.052	24	0.41	1.63
	0.087	54	0.24	0.97
3	0.066	1210	0.48	1.93
	0.100	96	0.32	1.27
	0.136	45	0.23	0.94
4	0.079	6940	0.54	2.15
	0.115	326	0.37	1.48
	0.149	61	0.29	1.14
	0.185	40	0.23	0.92
5	0.092	4.2×10^4	0.58	2.31
	0.129	1380	0.41	1.65
	0.163	157	0.33	1.30
	0.197	47	0.27	1.07
6	0.104	2.6×10^5	0.61	2.44
	0.142	6360	0.45	1.79
	0.177	535	0.36	1.44
	0.211	97	0.30	1.20
	0.246	39	0.26	1.03
7	0.116	1.7×10^6	0.64	2.55
	0.155	3.1×10^4	0.48	1.91
	0.191	2050	0.39	1.55
	0.226	276	0.33	1.31
	0.260	69	0.29	1.14
	0.295	34	0.25	1.00
8	0.129	1.1×10^7	0.66	2.64
	0.168	1.6×10^5	0.50	2.01
	0.205	8400	0.41	1.65
	0.240	917	0.35	1.41
	0.274	169	0.31	1.24
	0.308	53	0.27	1.10
	0.344	32	0.25	0.99

On the other hand a disturbance, such as the sinusoidal one considered by Longuet-Higgins, that continually feeds energy onto the sill for a period of time long compared with the damping factors *and* the minimum record length required may make itself felt at the island. One of Longuet-Higgins' diagrams is reproduced here as Figure 8. It shows the squared-amplitude response in comparative units of the sill system to a sinusoidal disturbance as a function of its frequency. The abscissal axis has been re-plotted in units appropriate to Norfolk I. If the disturbance is a superposition of a broad band of frequencies, then Figure 8, modified by the energy density

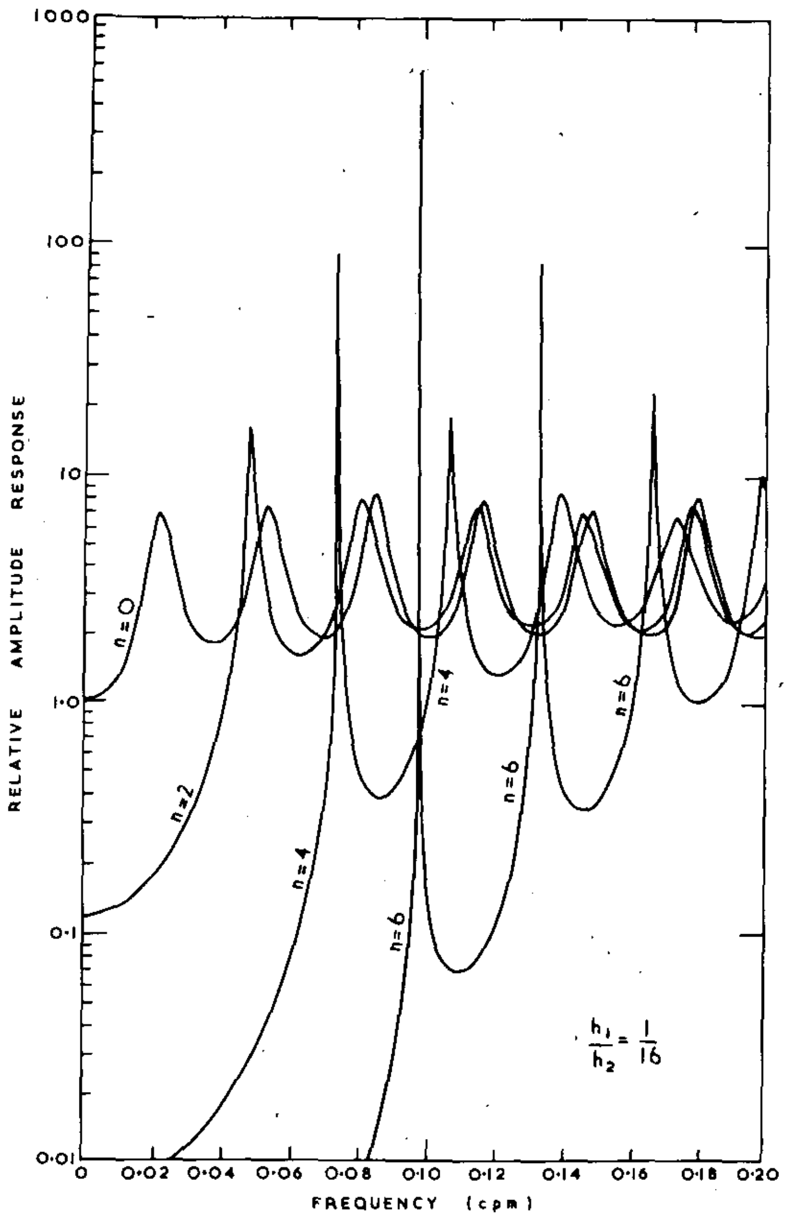

Fig. 8.–The amplitudes of the even-numbered modes on the sill in response to an incident plane wave as a function of frequency. The frequency units are those appropriate to Norfolk I. (Adapted from Longuet–Higgins 1967.)

distribution $E_\infty(\omega)$ of the disturbance, shows the spectral response of the sill. The high amplitudes of the resonant peaks in Figure 8 are illusory from the point of view

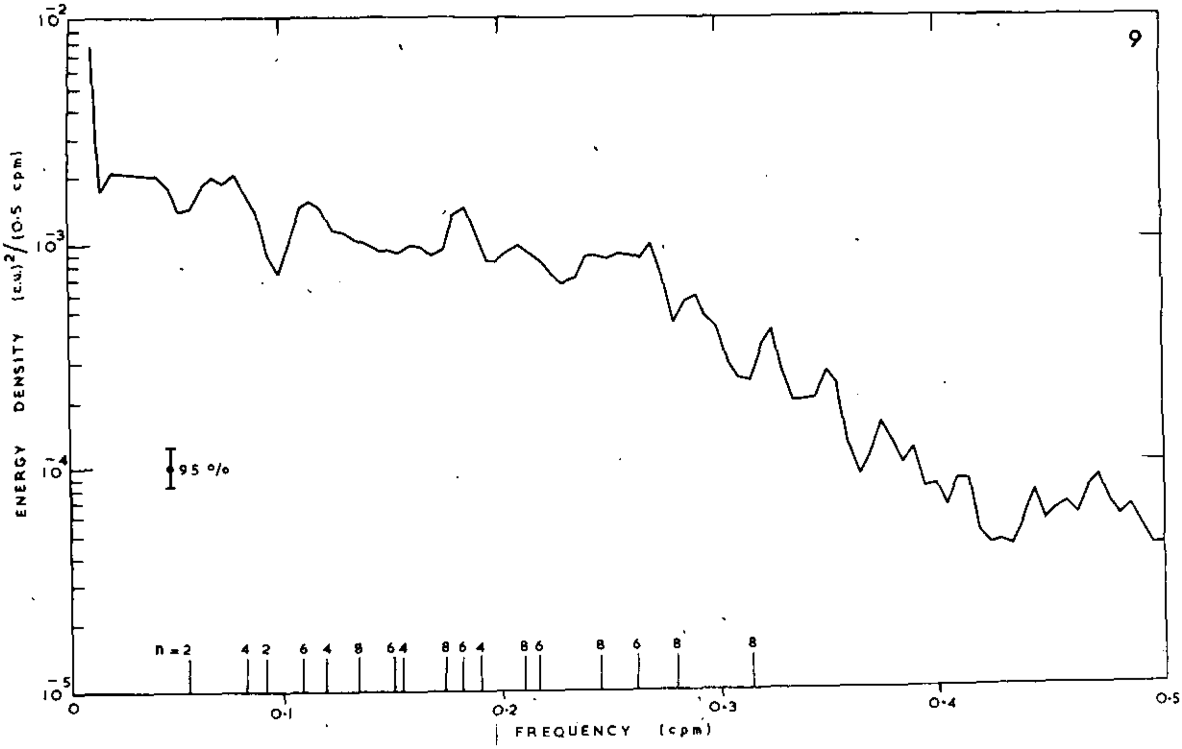
9
ENERGY DENSITY (c.u.)²/(0·5 cpm)
FREQUENCY (cpm)
95 %
n = 2
0
0·1
0·2
0·3
0·4
0·5

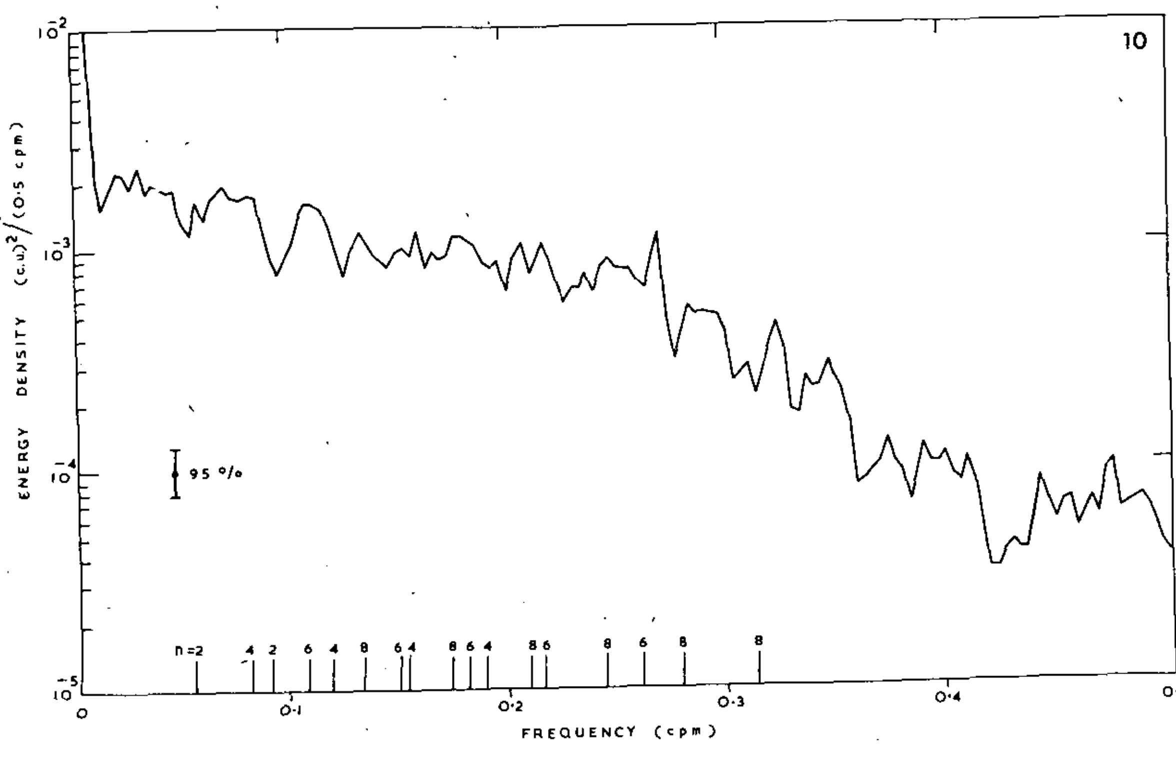
10
ENERGY DENSITY (c.u.)²/(0·5 cpm)
FREQUENCY (cpm)
95 %
n = 2
0
0·1
0·2
0·3
0·4

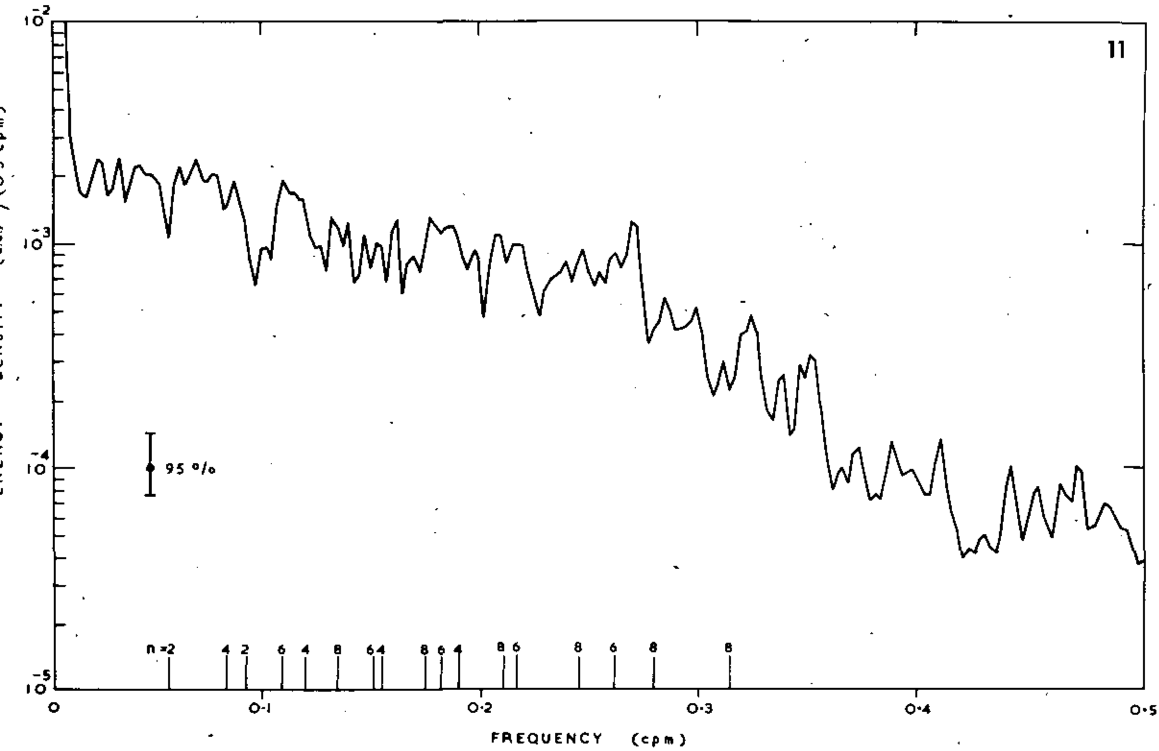

Figs. 9–11.—Spectra of period 0931 hr February 12, 1958, to 0927 hr February 18, 1958, for frequency resolutions of 0.0025 cpm (Fig. 9), 0.0033 cpm (Fig. 10), and 0.005 cpm (Fig. 11). Also shown are the frequencies of the even trapped modes labelled by their polar wave number n, and the 95% confidence limits.

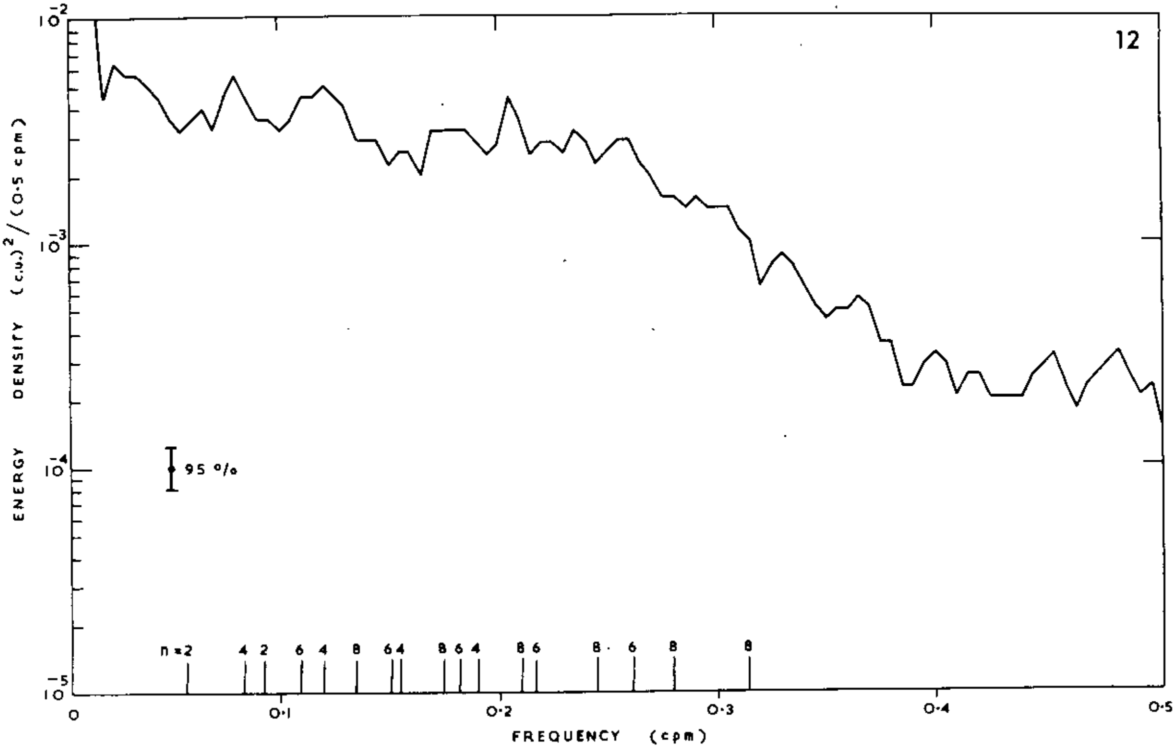
12
ENERGY DENSITY (c.u.)^2/(0·5 cpm)
10^{-2}
10^{-3}
10^{-4}
10^{-5}
95 %
n = 2 4 2 6 4 8 6 4 8 6 4 8 6 8 6 8 8
0 0·1 0·2 0·3 0·4 0·5
FREQUENCY (cpm)

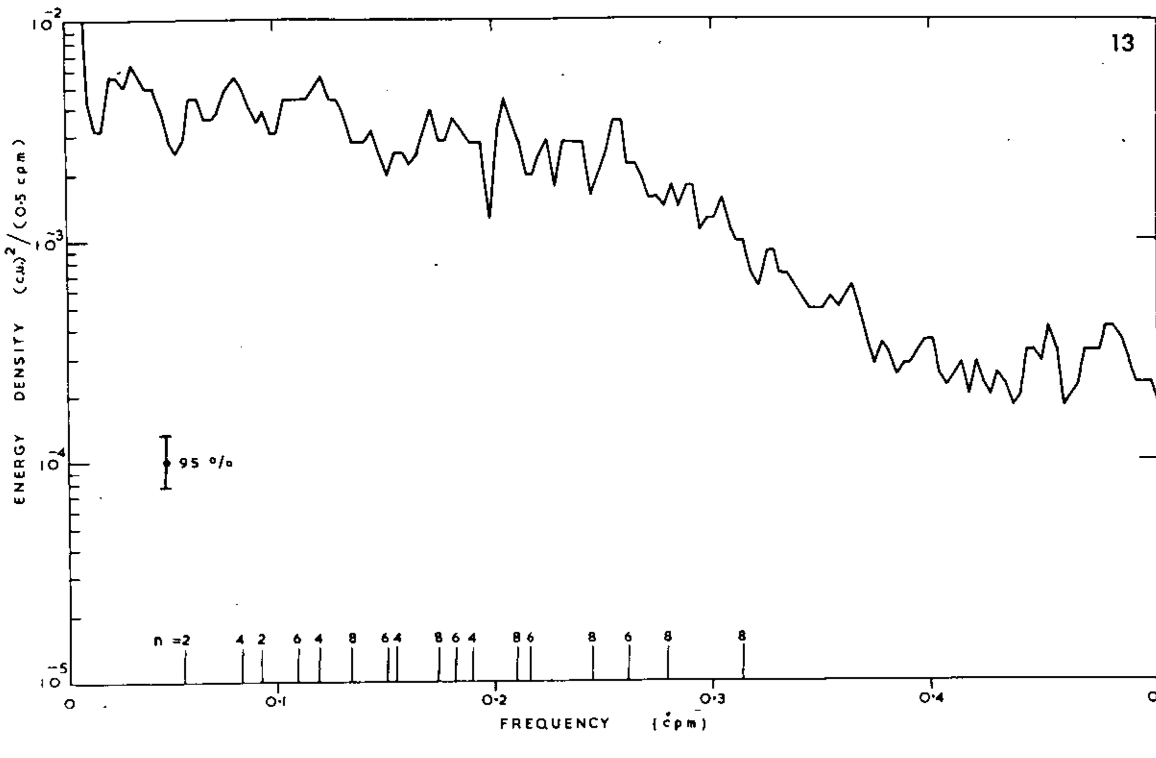
13
ENERGY DENSITY (c.u.)^2/(0·5 cpm)
10^{-2}
10^{-3}
10^{-4}
10^{-5}
95 %
n = 2 4 2 6 4 8 6 4 8 6 4 8 6 8 6 8 8
0 0·1 0·2 0·3 0·4
FREQUENCY (cpm)

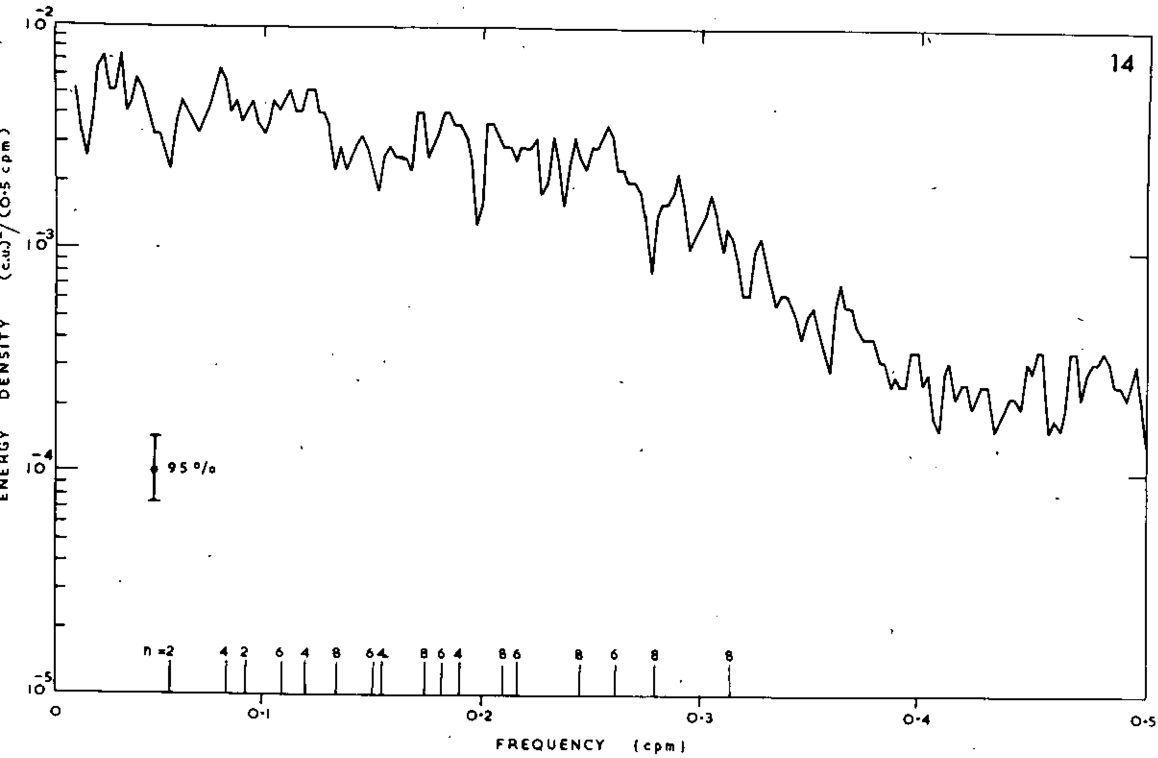

Figs. 12.–14.–Spectra of period 1546 hr March 17, 1958, to 0230 hr in March 23, 1958, for frequency resolutions of 0.0025 cpm (Fig. 12), 0.0033 cpm (Fig. 13), and 0.005 cpm (Fig. 14). Also shown are the frequencies of the even trapped modes labelled by their polar wave number n, and the 95% confidence limits.

of spectral analysis because such an analysis estimates an *average* spectral density over a small band of frequency whose width is chosen for statistical reliability. As Longuet-Higgins notes, the comparative spectral density averaged over the band width of the resonant peaks is necessarily of order unity. Thus, if the band width over which the spectral estimates are averaged is greater than or comparable to the band width of the peak (defined by Longuet-Higgins as the frequency interval between the half peak amplitudes on either side) we expect the analysis to smooth over the resonances of the island sill and simply to represent the broad-band spectrum of the disturbing influence. This is the case for the 6-hourly spectra with 36 spectral estimates described in previous sections. For these the band width between estimates is 0.0139 cpm and comparable to the band widths of the peaks in Figure 8.

Hence, in spite of the previous strictures regarding non-stationarity over long pieces of record, continuous lengths of maximum duration (i.e. several days) were analysed to obtain respectively 100, 150, and 200 spectral estimates in the 0–0.5 cpm range with acceptably narrow confidence limits. The band widths over which the estimates are made are then 0.005, 0.0033, and 0.0025 cpm. These narrow widths are ample to distinguish trapped island modes if such modes persist for a long enough period of time at a level higher than the background activity.

Two pieces of record were so analysed: from 0931 hr February 12, 1958, to 0927 hr February 18, 1958, and from 1546 hr March 17, 1958, to 0230 hr March 23, 1958. The results are shown in Figures 9–14, together with the 95% confidence limits. Indicated on the abscissal axis are the frequencies of the trapped island modes. No fine structure significant at the 95% level is discernible in these spectra. The most striking features in the spectra are similar to ones which are evident in the 6-hourly spectra: a fairly constant level of activity from 0 to 0.27 cpm, a relatively abrupt drop between 0.27 and 0.38 cpm, then another plateau from 0.38 to 0.5 cpm. Certainly nothing which could unambiguously be attributed to island trapping is apparent. However, this is a result not inconsistent with the theoretical reasoning above.

V. Impulsive Generation of Ridge Waves

Norfolk I. is a relatively small protuberance at the centre of an otherwise fairly flat-topped guyot. This geometry has led to the hypothesis of island sill-trapping (see Section IV). However, on a larger scale, the Norfolk I. guyot sits on a ridge running approximately north–south from New Zealand to New Caledonia. Characteristically, this ridge is of depth $h_1 = 1000$ m (with a width of $2a = 80$ km) rising from surrounding water of depth $h_2 = 4000$ m. This ridge can support trapped shelf waves of the type discussed by Snodgrass, Munk, and Miller (1962) and Buchwald (1968), and observed by Munk, Snodgrass, and Gilbert (1964). The dispersion relationship for these waves is

$$m^2 = \omega^2 - k^2, \quad r^2 = k^2 - \omega^2/\mu^2 \quad (r>0), \quad \mu = (h_2/h_1)^{1/2}$$

$$m \tan m = \mu^2 r \text{ for } \tfrac{1}{2}j\pi < m < \tfrac{1}{2}(j+1)\pi, \quad j = 0, 2, 4, 6, \ldots\ldots \tag{4a}$$

and

$$m \cot m = -\mu^2 r \text{ for } \tfrac{1}{2}j\pi < m < \tfrac{1}{2}(j+1)\pi, \quad j = 1, 3, 5, \ldots\ldots \tag{4b}$$

where $\lambda = 2\pi/k$ is the apparent along-shelf wavelength in units of the half-shelf width

a, and $\tau = 2\pi/\omega$ is the wave-period in units of the time taken $a/(gh_1)^{1/2}$ for a long wave to cross half the ridge. The modes for even j are symmetrical about the centre of the ridge, and those for odd j are antisymmetrical.

These modes are plotted for $\mu = 2$ in Figure 15 in units of frequency and wave-number appropriate to the Norfolk ridge. Only the first few even modes are plotted. Each branch of the dispersion relation has an inflexion $\omega''(k) = 0$ at which a minimum group velocity $\omega'(k)$ is attained. These points are also marked on Figure 15 for $j = 0(1)9$ and listed in Table 4.

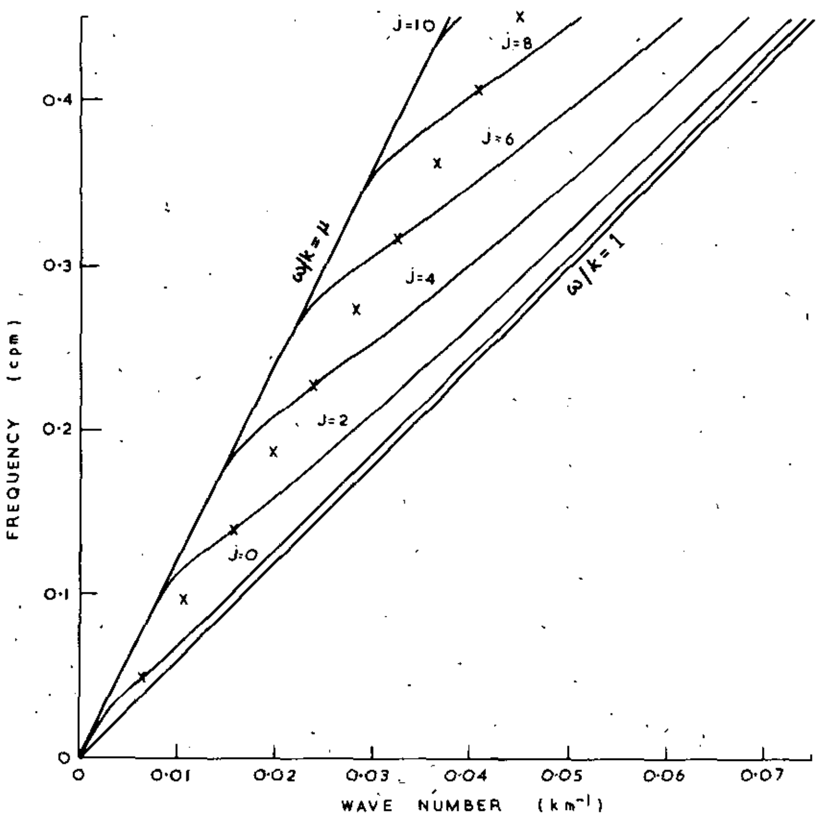

Fig. 15.–The even modes of the dispersion relation for a ridge with $h_1/h_2 = 1/4$ ($\mu = 2$). Frequency and wave number units are those appropriate to Norfolk I. The crosses mark the inflexion points (minimum group velocity) on each mode for $j = 0(1)9$.

Consider the impulsive generation of waves on the ridge at time $t = 0$ by a meteorological disturbance such as a storm, typically 100–200 km in size, crossing the ridge at a point distant x (in units of a) from the island. The dispersion relation (4) is essentially one-dimensional, so we can apply Jeffreys and Jeffreys (1956, Section 17.08) formalism for one-dimensional impulsive generation. They have derived, for the response of a channel, in which a dispersion relation $\omega = \omega(k)$ is known, to a unit step-function impulse at $t = 0$, the following asymptotic formula

$$\zeta \sim \sin(\omega_0 t - k_0 x - \tfrac{1}{4}\pi \operatorname{sgn} \omega_0'')/[(2\pi|t\omega_0''|)^{1/2} k_0] \tag{5}$$

where k_0 is such that

$$\omega_0' \equiv \omega'(k_0) = x/t, \quad \omega_0'' \equiv \omega''(k_0), \tag{6}$$

i.e. that wavenumber whose group velocity ω_0' is just sufficient to reach the island in time t available.

TABLE 4

INFLEXIONS OF DISPERSION RELATION FOR MODES $j = 0(1)10$ WITH CORRESPONDING MINIMUM GROUP VELOCITIES

Mode	Frequency (cpm)	Wave Number (km^{-1})	Group Velocity (km/hr)
0	0.050	0.0065	316
1	0.095	0.0112	292
2	0.140	0.0157	278
3	0.185	0.0201	268
4	0.230	0.0244	261
5	0.274	0.0286	256
6	0.318	0.0327	252
7	0.363	0.0378	248
8	0.408	0.0410	244
9	0.452	0.0450	242
10	0.496	0.0490	238

Graphically, the response of the system to an impulse may be understood as follows. As t increases the ratio x/t decreases and each branch (or mode) of the dispersion relation contributes that wave number and frequency at which the slope is equal to x/t. Thus, if $t < x/\mu$ ($x/t > \mu$), no modes are possible (see Fig. 15): this is because μ, the free phase velocity of long waves in the deep water, cannot be exceeded by any mode. When t equals x/μ the longest wavelengths and periods from each mode appear at the island and as x/μ is exceeded these wavelengths and periods shorten. As t increases past x ($x/t = 1$, the long-wave phase velocity on the shelf) a second wavelength period pair become possible in each mode at the short period end. As t increases further the minimum group velocities at which maximum amplitudes occur are reached. These amplitudes are maxima because of $(\omega_0'')^{1/2}$ in the denominator of (5). As Table 4 shows, the 0th mode's minimum group velocity is reached first, followed by the first mode, second, etc. However, these minima are quite close in value and will be reached in rapid succession. Beyond the minimum group velocities there are no real solutions of $\omega'(k) = x/t$ and the group dies out.

Consider a hypothetical storm on the Norfolk I. ridge 2000 km from the island. The deep-water, long-wave phase velocity is $(gh_2)^{1/2} = 720$ km/hr and the ridge long-wave velocity is $(gh_1)^{1/2} = 360$ km/hr. Thus, very long period activity may be felt initially after 2.8 hr, augmented at 5.6 hr after the storm. The 0th mode's maximum activity is reached shortly thereafter at 2000/316 = 6.3 hr (period = 20 min), the fifth's at 2000/256 = 7.8 hr (period = 3.6 min), and the tenth's at 2000/238 = 8.4 hr (period = 2.0 min). The amplitudes of the modes are proportional to the wavelengths $2\pi/k_0$ (see equation 5) so that the higher modes become less and less important. Munk, Snodgrass, and Gilbert (1964), working on a continental shelf where only the even modes can occur, detected vestiges of the sixth mode.

Hence, we have the following picture of the arrival of a group of ridge waves impulsively generated by a distant storm: the maximum amplitudes of the group pass within about 2 hr, the wave periods shortening by an order of magnitude from 20 to 2 min during this space of time; the amplitudes die off in inverse proportion (approximately) to the wave periods. I have examined two instances of sudden high activity in the records, one occurring between 0330 and 0900 hr, February 19, 1958, the other between 1500 hr March 17, 1958, and 0600 hr March 19, 1958. The duration of the first group is rather long to be explained by impulsively generated ridge waves, the second group is far too long. Moreover, both occasions exhibited wave periods visually estimated at 3–6 min with no shortening at all of the periods with time. We conclude that these groups were not cases of impulsively generated ridge waves, nor is it likely that any of the other instances of high activity in the records are ridge waves as none show what should be their most marked characteristic, the shortening of the periods towards the rear of the group.

Actual storms are expected to influence the ridge while they are close to it (i.e. within one wavelength distant) during approach or while receding, and while they pass over it. Now the wavelength of the fundamental (longest) ridge mode is approximately twice the ridge width so that, for the Norfolk I. ridge of width 80 km, influence may be exerted over $5 \times 80 = 400$ km. Assuming an east-to-west speed of progression for the storm of about 50 km/hr this influence extends over 8 hr. Although this estimate is very approximate, clearly the duration of the influence of the storm is much longer than the wave periods one expects to observe (< 20 min).

This suggests that the notion of "impulsive" generation by storms is false. However the term "impulsive" in our description of Jeffreys and Jeffreys' mechanism refers not to the duration of the disturbance but to its rate of onset. In a similar vein, Van Dorn (1965) has studied the generation of a tsunami by the sudden dislocation of a piece of the ocean floor. If the original configuration of the ocean floor were restored, the first tsunami would be followed by an exactly similar one except for a complete amplitude inversion (i.e. crests in the first tsunami will correspond to troughs in the second, for obvious reasons). Similarly, in our situation, we expect the onset of the storm to generate a group of ridge waves as described above, followed by a second group after the passage of the storm.

In Jeffreys and Jeffreys' treatment the onset of the storm is instantaneous (a step-function) which is what is meant by "impulsive". The Fourier spectrum of a step-function behaves like $1/\omega$ (or $1/k$) which explains the occurrence of this factor in the subsequent response (5) of the water. In fact, the onset of the storm is more gradual, so that its Fourier spectrum attenuates much more markedly for high frequencies ω: for example, if the build-up to the storm is linear in time, its Fourier spectrum behaves like $1/\omega^2$. In this case the attendant response of the ridge waves is similarly attenuated.

In the real situation, therefore, we expect the higher frequencies to be discriminated against even more markedly than formula (5) suggests. However, in the observed wave groups, the visually estimated period range is 3–6 min against 20 min for the theoretically most favoured period in the fundamental mode.

If the observations are to be explained by storm generation of ridge modes, an alternative mechanism must be sought: perhaps one which can generate waves continually while the storm is on or near the shelf in order to explain the comparably long duration of the observed groups; also one with an unusual Fourier spectrum to explain the peculiar observed distribution of wave frequencies.

VI. Discussion and Conclusions

As no positive unambiguous conclusions could be drawn from the analysis and interpretation of the wave records at Norfolk I., the principal value of this work lies in the suggestions that can be made for any future investigations.

The original purpose of the installers of the instrument was to observe long-wave activity associated with seismic activity. This was unsuccessful because long waves are non-dispersive in the open ocean and wave groups associated with only a moderate impulsive disturbance will pass too quickly to be noticed. Our intention in analysing the data was to investigate the occurrence of circular sill waves at the island. This was unsuccessful and inconclusive because the recorder was located at the island, the centre of the sill and theoretical nadir of sill-wave activity. Optimum results would be obtained from a recorder near the inner critical radii of the modes: in the case of Norfolk I. this would be at about 20 km distance from the island. An array of three recorders (perhaps even two) separated by 2–3 km in this critical region situated north or south of the island would be able to discern the directions of the wave components and so distinguish sill waves swinging around the island from ridge waves travelling north–south along the ridge and from long-wave groups travelling across the open ocean and running up on to the sill. These latter would be more marked in amplitude at the island shore itself because of set-up (Longuet-Higgins and Stewart 1962, 1964). A long-wave recorder should be operated in conjunction with a swell recorder at the island in order to check for the occurrence of surf beat.

The best method for discerning ridge waves is to attempt to verify the dispersion relation (4) as has been done by Munk, Snodgrass, and Gilbert (1964) who leap-frogged three wave recorders at spacings of less than 1 km along about 30 km of coast to obtain both spatial and time transforms of the data. However, this is probably not practical at Norfolk I. because of its rugged terrain.

Finally, note should be taken of all meteorologic disturbances which could generate long-wave activity, especially severe storms or cyclones which cross the Norfolk I. ridge at any point. Air pressure and anemometer wind records should be made at the island to check for any as yet unknown local mechanisms of long-wave generation.

These suggestions all carried out together would form a program for the optimal solution of the problem. However, if preferred, any single aspect of long-wave activity, such as surf-beating for instance, could be selected and investigated with only that part of the program necessary for its solution.

VII. Acknowledgment

We wish to thank Professor J. C. Jaeger, Department of Geophysics, Australian National University, Canberra, for making the records available for analysis.

VIII. REFERENCES

Buchwald, V. T. (1968).–Long waves on oceanic ridges. *Proc. R. Soc.* A **308**, 343–54.

Groves, G. W., and Hannan, E. J. (1968).–Time series regression of sea level on weather. *Rev. Geophys.* **6**, 129–74.

Holsten, W. G., and Groves, G. W. (1966).–A system of macro programs for time series analysis. *Hawaii Inst. Geophys.* HIG–66–10.

Jeffreys, H., and Jeffreys, B. S. (1956).–"Methods of Mathematical Physics." 3rd Ed. (Cambridge Univ. Press.)

Jaeger, J. C. (1960).–Long ocean waves. *Aust. J. Sci.* **23**, 4–9.

Longuet-Higgins, M. S. (1967).–On the trapping of wave energy round islands. *J. Fluid Mech.* **29**, 781–821.

Longuet-Higgins, M. S., and Stewart, R. W. (1962).–Radiation stress and mass transport in gravity waves with application to 'surf beats'. *J. Fluid Mech.* **13**, 481–504.

Longuet-Higgins, M. S., and Stewart, R. W. (1964).–Radiation stress on water waves; a physical discussion with applications. *Deep Sea Res.* **11**, 529–62.

Miller, G. R., Munk, W. H., and Snodgrass, F. E. (1962).–Long period waves over California's Continental Borderland. Pt. II. Tsunamis. *J. Mar. Res.* **20**, 31–41.

Munk, W. H. (1949).–Surf beats. *Trans. Am. Geophys. Un.* **30**, 849–54.

Munk, W. H., Iglesias, H. V., and Folsom, T. R. (1948).–An instrument for recording ultra low frequency ocean waves. *Rev. scient. Instrum.* **19**, 654–8.

Munk, W. H., Miller, G. R., Snodgrass, F. E., and Barber, N. F. (1963).–Directional recording of swell from distant storms. *Phil. Trans. R. Soc. Lond.* A **255**, 505–84.

Munk, W. H., Snodgrass, F. E., and Gilbert, F. (1964).–Long waves on the continental shelf: an experiment to separate trapped and leaky modes. *J. Fluid Mech.* **20**, 529–54.

Newman, B. W., and Bath, A. T. (1959).–Occurrence of tropical depressions and cyclones in the north-eastern Australian region during the season 1957–1958. *Aust. Met. Mag.* **24**, 35–64.

Rosenblatt, M. (1962).–"Random Processes." ch. 7. (Oxford University Press : New York.)

Snodgrass, F. E., Munk, W. H., and Miller, G. R. (1962).–Long period waves over California's Continental Borderland. Pt. I. Background spectra. *J. Mar. Res.* **20**, 3–30.

Stacey, F. D. (1961).–Oceanographic work at stations in the Australian territories. *Aust. Territories* **1**(3), 32–6.

Summerfield, W. (1967).–On the six minute period wave phenomenon recorded at Macquarie Island. Res. Pap. Horace Lamb Centre Oceanogr. Res. No. 16.

Tucker, M. J. (1950).–Surf beats: sea waves of 1 to 5 min. period. *Proc. R. Soc.* A **202**, 565–73.

Van Dorn (1956).–A portable tsunami recorder. *Trans. Am. Geophys. Un.* **37**, 27–30.

Van Dorn (1965).–Tsunamis. *Adv. Hydrosci.* **2**, 1–48.

DIVISION OF FISHERIES AND OCEANOGRAPHY
TECHNICAL PAPERS

1. Blackburn, M., and Rayner, G. W. (1951).—Pelagic fishing experiments in Australian waters.
2. Houston, T. W. (1954).—Commercial trawling tests in the Great Australian Bight, 1949–52.
3. Blackburn, M., and Downie, R. J. (1955).—The occurrence of oily pilchards in New South Wales waters.
4. Weatherley, A. H. (1958).—Tasmanian farm dams in relation to fish culture.
5. Dunstan, D. J. (1959).—The barramundi *Lates calcarifer* (Bloch) in Queensland waters.
6. Jitts, H. R. (1959).—Measurements of light penetration in the Tasman Sea, 1955–57.
7. Rochford, D. J. (1959).—The primary external water masses of the Tasman and Coral seas.
8. Wyrtki, K. (1960).—The surface circulation in the Coral and Tasman seas.
9. Humphrey, G. F. (1960).—The concentration of plankton pigments in Australian waters.
10. Newell, B. S. (1961).—Hydrology of south-east Australian waters: Bass Strait and New South Wales tuna fishing area.
11. Hamon, B. V. (1961).—The structure of the East Australian Current.
12. Wisely, B., and Purday, C. (1961).—An algal mass-culture unit for feeding marine invertebrate larvae.
13. Thomson, J. M. (1962).—The tagging and marking of marine animals in Australia.
14. Wood, E. J. F. (1963).—Dinoflagellates in the Australian region. II. Recent collections.
15. Hamon, B. V. (1963).—Australian tide recorders.
16. Thomson, J. M. (1963).—A bibliography of systematic references to the grey mullets (Mugilidae).
17. Wood, E. J. F. (1963).—Dinoflagellates in the Australian region. III. Further collections.
18. Dyson, N., Jitts, H. R., and Scott, B. D. (1965).—Techniques for measuring oceanic primary production using radioactive carbon.
19. Tranter, D. J. (1966).—The Australian Clarke–Bumpus sampler and calibration tank.
20. Wisely, B. (1966).—Application details and sea-trial results of an antifouling and anticorrosion system.
21. Castillejo, F. F. de (1966).—Non-seasonal variations in the hydrological environment off Port Hacking, Sydney.
22. Hynd, J. S., and Robins, J. P. (1967).—Tasmanian tuna survey. Report of first operational period.
23. Highley, E. (1967).—Oceanic circulation patterns off the east coast of Australia.
24. Kesteven, G. L., and Stark, A. E. (1967).—Demersal fish stocks of the Great Australian Bight as estimated from the results of operations of F.V. *Southern Endeavour*.
25. Kirkwood, L. F. (1967).—Inorganic phosphate, organic phosphorus, and nitrate in Australian waters.
26. Hynd, J. S. (1968).—Report on a survey for yellowfin tuna, *Thunnus albacares* (Bonnaterre), in Queensland waters.
27. Highley, E., and Stark, A. E., (1968).—The Great Australian Bight and trawling tests of F.V. *Southern Endeavour*.
28. Highley, E. (1968).—The International Indian Ocean Expedition: Australia's contribution.
29. Rochford, D. J. (1969).—The seasonal interchange of high and low salinity surface waters off south-west Australia.
30. Newell, B. S. (1970).—The hydrological environment of Moreton Bay, Queensland.
31. de Szoeke, R. A. (1972).—Long waves at Norfolk Island.